Preliminary Damage Severity Evaluation of Ground Vehicles and Covered Walkways under Collision with a Small Unmanned Aerial Vehicle (sUAV)

Mohd Hasrizam Che Man[1], Haoliang Hu[2], and Anush Kumar Sivakumar[3],
Air Traffic Management Research Institute, Nanyang Technological University, 637460, Singapore

Kin Huat Low[4]
School of Mechanical and Aerospace Engineering, Nanyang Technological University
639798, Singapore

It is expected that the use of small drones will increase in urban areas in the future for different purposes such as package delivery, industrial inspection, aerial photography, and security surveillance. However, the increase in sUAV traffic may increase the chance of sUAV failure, and debris from air collisions may fall and endanger the safety of vehicles and pedestrians on the ground. The Finite Element Method (FEM) was employed to simulate and evaluate the severity of damage caused by a collision of sUAV (DJI Phantom III and generic multi-rotor UAV weight) to the windshield and roof cover of the car and covered walkway. Moreover, a series of collision simulations were carried out with different parameters such as crash speeds of the sUAV and driving speeds of the car to study the effect of speeds on the severity of damage to the ground vehicles. It was found the damage severity level of car windshield due to drone crash at higher car forward speed cause more severe damage for same weight category. Further analysis of car roof and covered walkway failure due to sUAV operation also be studied, and the simulation shows no damage to the structures was noticed. However, further study with heavier UAVs is recommended to be performed in the future to have a better understanding of this risk. Insights from this study will guide aviation airworthiness authorities to better understand the damage severity level to land vehicles due to sUAV collisions. At the same time, this will facilitate aviation authorities to formulate regulations for safer sUAV operations.

I. Introduction

The use of sUAV has attracted a lot of attention due to its potential for different applications, such as parcel delivery, industrial inspection, and urban air mobility. However, the risk associated with the drone operation in such environment still has not been fully understood, especially for operations within an urban environment and near aerodrome airspace. Currently, regulatory bodies such as FAA [1] have restricted a small UAV weight of less than 25 kg should be operated 5 km from aerodrome airspace, under Visual Line-of-Sight (VLOS) and not above the crowd. There are many studies on the safety threats of drones to manned aircraft and pedestrians; however, there is also a

[1] Research Associate, Air Traffic Management Research Institute
[2] Graduate Student, School of Mechanical and Aerospace Engineering
[3] Project Officer, Air Traffic Management Research Institute
[4] Professor, AIAA Member; Corresponding author: mkhlow@ntu.edu.sg

certain threat for ground vehicles. The traffic accident caused by UAV collision has been increasing sharply in recent year, which pose a certain threat to the safe driving of ground vehicles [2]. Current research on the assessment of damage to the automobile due to collisions with a sUAV is extremely limited, which has great exploration space and exploration value.

However, there are few research reports on collisions between UAVs and cars. When small UAVs operating in urban areas fail, one of the most serious hazards can be collisions with vehicles and pedestrians on the ground. Polyvinyl butyral (PVB) laminated glass is the main material of choice for windshields in the automotive industry today, and it is more vulnerable to the impact of crashing UAVs than other automotive components while it is also more fragile.

PVB laminated glass is usually composed of two or more layers of glass plates sandwiched on one or more layers of PVB. When UAVs penetrate windshields, it will pose a serious threat to the people in the vehicle; even penetration does not occur. The damage to visibility will also make cars lose control and bring serious life and safety threats to people driving cars. Although this fatal risk has been recognized, there are few studies on the risk assessment of the impact of drones on glass [3]. The laminated glass window used in an automobile is nominally 4.76 mm thick, with two 2.0 mm thick glass plates interlayered with 0.76 mm thick PVB gluing [4, 5]. In this study, damage severity from a collision of sUAV with the windshield of cars at different relative speeds was evaluated using FEM analysis.

To simulate the real car windshield and the real small UAV, collision simulation was performed and validated with experiments carried out by different researchers. In the finite element simulation, under various impact conditions and impact speed of the UAV, it was possible to observe the glass breakage or non-breakage. From the results of these tests, a damage evaluation matrix for UAVs impacting manned aircraft windshields was proposed. This validated numerical model will help estimate the risk of death or damage to many different types of UAVs and car windshields due to structural impacts.

The summary of this article is as follows: in the introduction, the impact of sUAV and car windshields impact is studied. Next, the second section discusses in detail the methods used in this paper, including geometry, material properties and validation of the car windshield model explained in detail. Followed by several numerical simulations will be performed to determine the severity of damage to the windshield and roof of the ground vehicles and the covered walkway being impacted at different relative speeds. Finally, several conclusions and future works are presented in the final section.

II. Literature Review

Although few studies focused on the impact of the drone with ground vehicles and covered walkways, there have been some other studies about the UAVs impacts on other models like glass windows, airplane engines, wings, and vertical stabilizers in recent years. In 2020, European Union Aviation Safety Agency (EASA) [6] produced a report which included a review of worldwide literature relating to the assessment of drone strikes by analysis or test. The report showed that with an appropriate level of support testing, the dynamic FEM analysis method provides a credible method for modelling UAV collisions. The range of drone masses considered in all reviewed literatures show that the lowest is DJI Spark (0.3 kg) to DJI Inspire (3.4 kg). Most research groups applied a classification system to describe the levels of damage recorded/predicted because of drone collisions, and then EASA proposed Impact Effect Assessment (IEA), which was a series of damage levels related to the impact of different component zones as shown in Table 1.

Table 1 Damage levels of drone collisions to aircraft windshield [6]

	Low risk	**Medium risk**	**High risk**
The effect at the Components level	The windshield is undamaged. Small scratches.	Extensive damage to one or more transparent plies. Visibility compromised.	Penetration of UAS into the cockpit. Failure of Windshield structure.
Effect on Operations	No or limited damage. Non-significant loss of external visibility.	No Penetration, partial loss of visibility.	Penetration or total loss of visibility.

In 2020, a study by Liu et al. [7] reported the impact of a DJI UAV and the airplane's engine. The dynamic response of the UAV collision with the manned aircraft engine was simulated based on the Finite Element Method. Both damage of fan blades and the thrust loss of the engine core caused by the damage in the compressor core was considered.

In 2017, Sang et al. [3] used small commercial UAVs impacted into a series of glass plates at different speeds and different angles, and a simulation model of the UAV was then developed to simulate the impacts using FEM and verified by comparison with experimental results. The simulation results were in good agreement with the impact force and predicted damage of the physical test. However, these were all low-speed collision tests in which the drones were impacted onto the test glass plate at a velocity of 12.7 m/s. The results were not applicable to the crash damage assessment of the crashed drone on ground vehicles, but it seems that FEM can be a useful and affordable tool to estimate the impact results of the drone and the ground vehicles.

In recent years, many studies have conducted impact tests based on the automobile windshield glass. Holmquist et al. [7] proposed a constitutive model for glass calculation under large strain, high strain rate and high pressure, which gave the initial strength and damage based on factors such as pressure, strain rate, and softening. Herndon et al. [8] used a featureless head model to perform impact tests on two types of automobile side windshields (ordinary glass and PVB laminated glass) and obtained their load-displacement curves. The study preliminarily showed that PVB laminated glass had a great difference in performance from ordinary glass.

Wingren et al. [9] studied the mechanical properties of windshield glass under the impact of an adult head module. Under the condition of an impact velocity of 11.2 m/s (EuroNCAP standard), The influence of relative impact angle (70°～90°) and windshield shape on the mechanical properties of the windshield were studied. They concluded that the impact angle and curvature had a greater influence on the characteristics of the windshield, and the damage to the glass caused by the vertical impact was worst. Zhao [10] also conducted a simulation study on the impact of the human head model on windshield glass and constructed a finite element model based on the continuous damage model. This study used anisotropic elastic damage tensor and linear damage evolution law to simulate the expend process of the cracks of laminated glass.

Chen et al. [11] studied the drop hammer impact test of PVB laminated glass with the help of a high-speed photography system, and theoretically analyzed the different crack initiation and propagation mechanisms of the front and back cracks of the laminated glass, concluded that the cracking of the back glass was earlier than that of the front glass when the cracks of the front and back glass overlap.

III. Methodology of FEM Collision Simulation for Car Impact Damage Assessment

In a situation of a drone crashing into the car from the air, the primary protection from the impact for the driver and passengers are the windshield, the door, and the roof cover, as shown in Fig. 1. Since the structures surrounding the glass panel are stronger, the front and rear windshields of the car and the glass windows around the car are the regions to be considered in our study. In our research, we mainly consider the following two conditions where the sUAV impact at the front windshields, causing penetration and direct casualties, or the situation that make the driver's vision be blocked and then cause a serious ground traffic accident while the sUAV impact at the roof plate of the car, causing penetration and direct casualties. The FEM collision simulation methodology is as follows.

1. Firstly, simulation of sUAV on car windshield and car roof using FEM impact analysis to validate the material model of the windshield is capable of mimicking actual damage and failure of the windshield.
2. Secondly is to simulate drone collision on a car windscreen, car roof and covered walkway (different impact angle and relative impact speed) using the data from the simulation in step 1.
3. Lastly, conclusions will be drawn from the results in this step by comparing different drone speeds and crash angles. Three car speeds are considered (30, 50 and 90 km/h) to simulate impact at three driving car speeds (i.e., 30 km/h on the slow road, 50 km/h on the road, and 90 km/h on the highway).

A. Validation of Car Windshield and Car Roof Material Model

FEM simulation of adult head impact on the car windshield was performed to validate the material and simulation setup of the PVB laminated glass for further simulation. The impact simulation of the car windshield is validated by comparing the experiment done by Liu et al. [5] with the model used in the present simulation.

PVB Laminated glass is an integral laminated material that is permanently bonded with a transparent organic polymer intermediate film between glass layers after a certain special process. For windshield materials on automobiles, PVB (Polyvinyl Butyral or polyvinyl butyral) is the first choice for bonding organic polymers in the middle of laminated glass. The material parameter of the car roof is set to a homogeneous steel plate.

To simplify the simulation of car impact with sUAV in this study, a glass plane was cut from the front windshield of the car as the domain of interest, as shown in Fig. 1(b). The car windshield used in the study has dimensions of 1260 mm in length, 790 mm in height and 4.76 mm in thickness, as shown in **Error! Reference source not found.**(b). Similarly, the thickness of the PVB layer is 0.76 mm, and on both sides of the interlayer, the glass has an even thickness

distribution modeled using C3DR element with a total number of 298,812 elements. The details on the FEM model of car windshield as presented below in Fig. 2(a) and 2(c).

A similar condition is followed in the present FEM simulation, where a dummy head impacts the car windshield model directly. The dummy head model was built by an aluminum ball with a radius of 82 mm and a polyvinyl chloride hemispherical shell with a thickness of 13.9 mm as shown in and a total weight of 4.49 kg as shown in Fig. 2(b). Impactor was modeled using C3DR element with a total number of 8,346 elements. The contact between the impactor and glass layer is specified as 0.3 [12, 13]. The simulation with impact velocities of 8.0 m/s, 11.2 m/s and the impact angle of 90° were conducted and compared with experimental results by Liu et al. [5, 14].

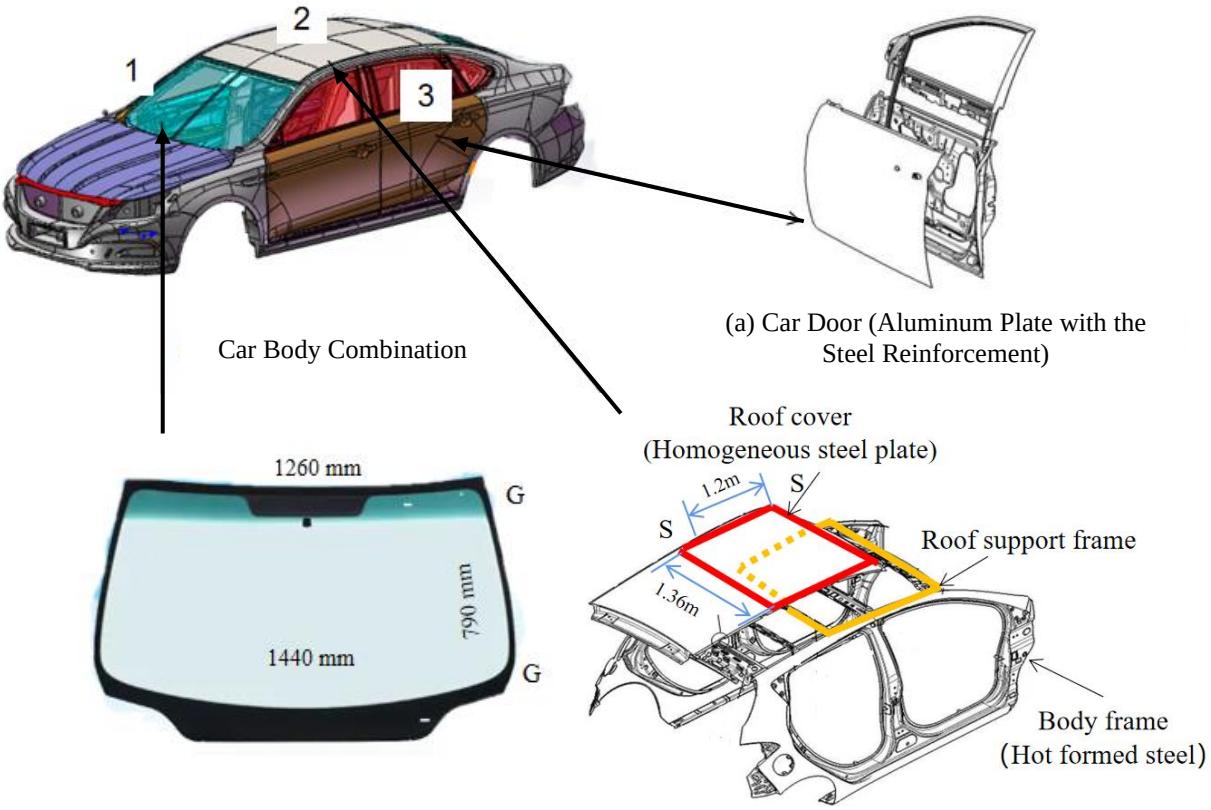

(b) Windshield (PVB laminated glass)

(c) Roof cover structure of a car

Fig. 1 Vehicle model used in the study (modified from [15]).

(a) Car windshield in present simulation

(b) Adult dummy head in the experiment

(c) Mesh of car windshield simulation model

Fig. 2 The windshield and head model in the experiment [5] and present simulation.

Due to the existence of the frame support frame in the car roof structure, as shown by the yellow box in Fig. 1(c), this study assumed that small UAVs are unable to cause damage to the car roof structure at low speeds. A homogeneous steel plate plane with a size of 1360 mm x 1260 mm x 0.8 mm (thickness) near the driver's seat on the support frame is selected as the domain of interest as depicted in Fig. 4(a) and Fig. 4(b). The finite element meshing sizes were set as 0.01-0.05 mm, as shown in Fig. 4(c). The roof fabric under the roof cover was not taken into consideration. GG (glass) shown in Fig. 1(b) represents the cross-sectional view dividing line of the glass window, and SS (steel) in Fig. 1(c) represents the cross-sectional view dividing line of the roof steel plate. Table 3 shows material properties defined in the collision simulation for the car roof.

Table 2 Material properties for car windshield [5]

Material	**Density, ρ**	**Young's Modulus, E**	**Poisson's ratio, υ**	**Direct stress after cracking**		**Failure strain, ε_f**
Glass	2600 kg/m^3	70 GPa	0.24	80.0 MPa		0.001 (0.1%)
Material	**Density, ρ**	**Young's Modulus, E**	**Poisson's ratio, υ**	**Yield stress, σ_y**	**Tangential Modulus, E_a**	**Failure strain, ε_f**
PVB	1100 kg/m^3	150 MPa	0.485	15.0 MPa	16.7 MPa	1.5 (150%)

Table 3 Material parameters for car roof [16].

Density, ρ	**Young's Modulus, E**	**Poisson's ratio, υ**	**Yield stress, σ_y**	**Ultimate Failure stress, σ_f**	**Failure strain, ε_f**
7800 kg/m^3	210.0 GPa	0.3	460 MPa	560 MPa	0.215 (21.5%)

The glass crack growth process of the windshield at different moments of the impact simulated by the present simulation and by the experimental analysis are compared in Table 4. From Table 4, it was found that the glass crack growth process predicted by the FEM simulation consists well with the experiment results, proving that the FEM model used in our study can accurately simulate the glass crack growth of windshield subjected to the impact loading.

Table 4 Comparison of the cracks process predicted by present simulation and experimental [5, 14]

Time	*t*=2ms	*t* =3ms	*t* =10ms	*t* =14ms
Experiment [5]				
Present Simulation	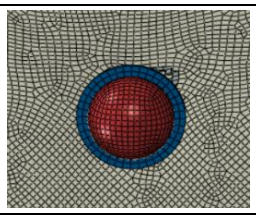	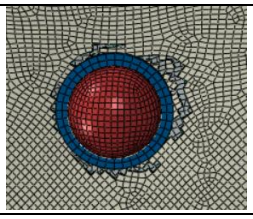	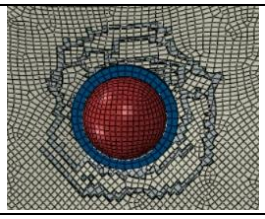	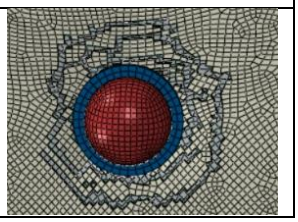

The time history of reaction force in 60 milliseconds obtained by experiment and present simulation are compared for speeds 8.0 and 11.2 m/s as shown in Fig. 3(a) and 3(b), respectively. The overall trend of the acceleration time change is relatively consistent. The simulation error mainly occurs in the process of glass rupture at the beginning of the collision. The acceleration curve does not reach the peak value consistent with the test, and there is a certain fluctuation. This is because the failure criterion is defined in FEA simulation, and when the element exceeds the maximum strength specified the element is deleted subsequently. The failure of the mesh affects the propagation of stress, which proves that the FEM model in our study can be well used to simulate and analyze the actual car windshield collision.

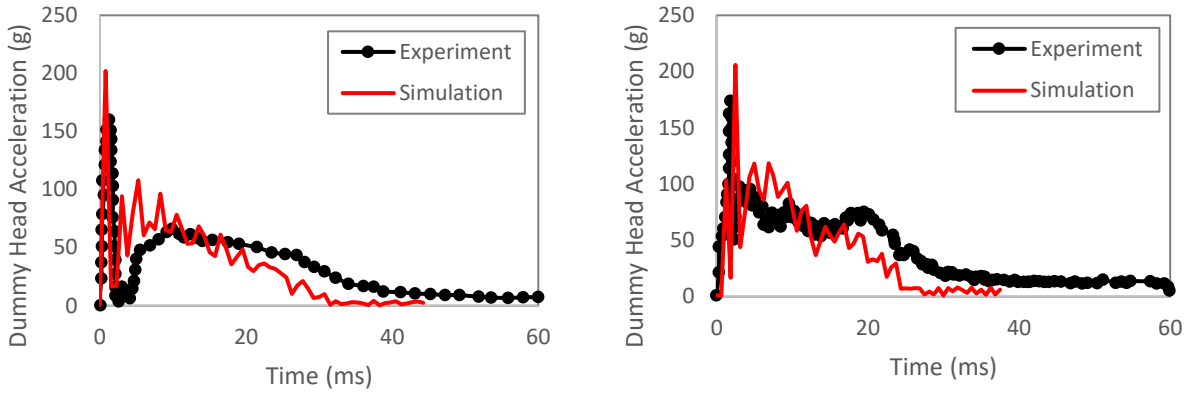

(a) 8.0 m/s (b) 11.2 m/s

Fig. 3 Acceleration of dummy head in experiment [5, 14] and present simulation.

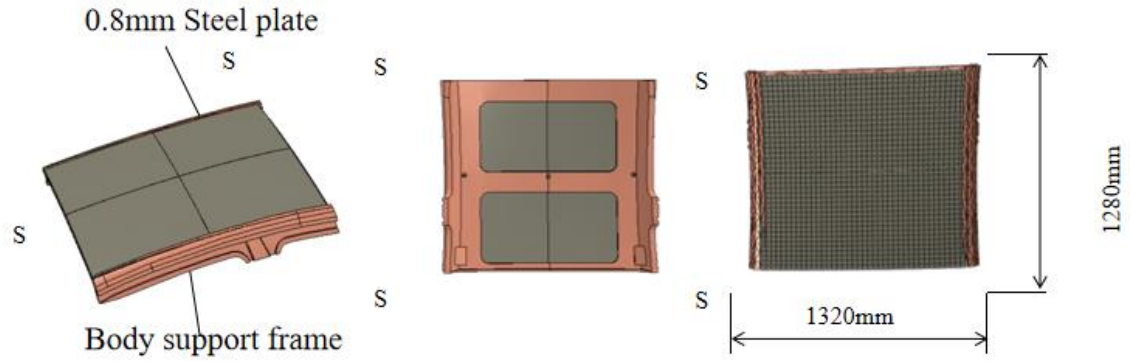

(a) roof cover model in abaqus (b) model bottom view (c) FE mesh model of roof cover

Fig. 4 Schematic diagram of PVB laminated glass: (a) 3D CAD car roof model in simulation, (b) 3D CAD bottom view car roof cover model in simulation, and (c) Finite element mesh model of car roof model.

B. Covered Walkway Material Model

A covered walkway is a sheltered pedestrian structure that constructed in Singapore to connect different buildings and major transport nodes, for example, to connect residential buildings to bus or Mass Rapid Transit (MRT) stations. Such structures covered quite a large ground area which could provide shelter to the pedestrians on the ground in case of sUAV faulty and crash. Therefore, assessing damage to covered walkways could provide insight into mitigation for sUAV operation in an urban environment.

To estimate the damage severity caused by the impact of sUAV, a typically covered walkway with a dimension of 2400 × 160 × 18.7 mm, as shown in Fig. 5, was considered in this study. The covered walkway dimensions are taken from Singapore Government Agency, Land Transport Authority (LTA) [17], where only the aluminum honeycomb panel, as depicted in Fig. 5(b), is to be considered in the present FEA simulation. The panel boundary condition is defined as pinned (i.e., fixed displacement fixed and free rotation) along all the edges.

Table 5 Material parameters for covered walkway [18]

Panel Section	Density, ρ	Young's Modulus, E	Poisson's ratio, υ	Yield stress, σ_y	Ultimate Failure stress, σ_f	Failure strain, ε_f
Aluminum face	2700 kg/m^3	70.0 GPa	0.33	117 MPa	124 MPa	0.45 (45%)
Aluminum core	2700 kg/m^3	70.0 GPa	0.33	220 MPa	250 MPa	0.45 (45%)

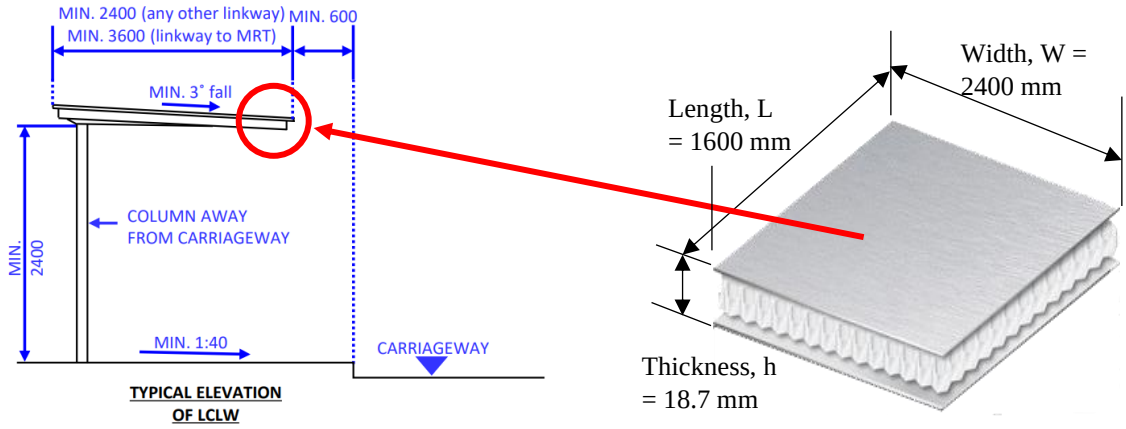

(a) schematic of a covered walkway (b) Aluminum honeycomb panel (not to scale)

Fig. 5 Schematic diagram of the covered walkway [17] and aluminum honeycomb panel considered in the FEA simulation.

C. Material Parameters of sUAV

To estimate the damage severity caused by the impact of sUAV, a typical micro-sized drone DJI PHANTOM 3 (dimension: 289.5 × 289.5 × 196 mm, weight:1.28 kg) was considered in this study. The UAV model is taken from previous studies [17], where the main components are to be considered, such as motors, battery, camera, main body, landing gear, electronic board, and propellers.

The materials used for sUAV are shown in Fig. 6, and the detailed material parameters are shown in

Table 6. To consider the thermal deformation and thermal damage of polycarbonate, steel and aluminum in high-speed impact, the Johnson-Cook failure model was added to material model in the simulation. The parameters of the Johnson-cook failure model are taken from the parameters used in study by Liu et al. [17].

Most parts of the UAV are meshed by hexahedron (C3D8 element type) with element size in range of 1.0~5.0mm, and the main body which has the thin-walled structures is meshed by shell element type S4, and the minimum element size is 1.0 mm, while the maximum element size is 2.0 mm.

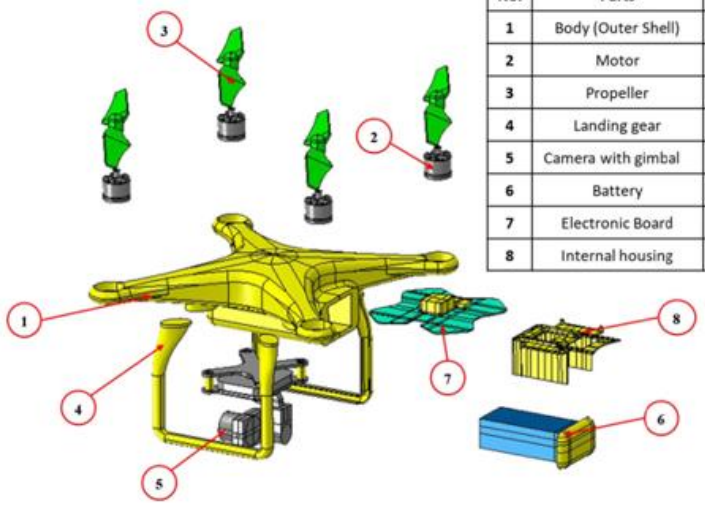

No.	Parts	Material
1	Body (Outer Shell)	PC
2	Motor	Al/Steel
3	Propeller	Nylon
4	Landing gear	PC
5	Camera with gimbal	Al
6	Battery	Li-Po
7	Electronic Board	FR-4
8	Internal housing	PC

Fig. 6 Schematic diagram of DJI PHANTOM 3 UAV model including components and material type.

Table 6 Material parameters in UAV model [17]

Material	Young's modulus (GPa)	Poisson's ratio	Yield stress (MPa)	Ultimate tensile stress (MPa)	Failure Strain (%)	Density (kg/m^2)
Steel	210	0.3	460	560	0.215	7800
Aluminum	66	0.33	170	330	0.14	2600
PC	2.59	0.37	50	50	0.5	1197.8
PC (body)	2.59	0.37	105	130	0.5	2197.8
Nylon	2.2	0.42	105	130	0.215	1340
Fiberglass	22	0.21	105	282	0.0195	1900
Li-Po	50	0.001	30	50	0.375	2600

D. Scenarios of Simulation sUAV crash on ground vehicles and covered walkway

Using ABAQUS software to carry out the FEM impact simulation of the sUAV and automobile, which was solved with Dynamic/Explicit formulation [19]. The overall simulation uses FEM (ABAQUS) to simulate the damage caused by the collision of the UAV to the vehicle. As shown in Fig. 7(a) and 7(b), the UAV and car assembly system for simulation is presented, in which the UAV will impact the moving car with an initial velocity (the relative velocity between UAV and car). Relative material properties, load conditions, and boundary conditions will also be provided for the UAV and car system. The damage results to the front and rear windshields of the car and the glass windows around can be estimated from the simulation results.

To simplify the calculation, the car roof and windshield (windows) are extracted separately, and the collision analysis is carried out in the form of parts of the same size extracted from the car from the impact of the UAV. At present, the speed limit of private cars in the urban area of Singapore is 50 km/h (13.9 m/s), and the speed has increased to 90 km/h (25 m/s) when it comes to the highway in Singapore. In the study, both two speeds will be considered to estimate the possible damage that crash UAVs will cause in different conditions on the road [20].

Considering the slope of the windshield when performing collision analysis on the laminated glass, we added the case of collision at an angle of 53°, as shown in Fig. 8(a). In several research studies on UAV crash trajectory [21-23], it was found that the angle at which the UAV impacted the ground is not fixed, but a considerable part of them is approximately at 90°. Therefore, in the collision analysis, the collision angle is selected as 90°, as shown in Fig. 8(b). The specific design of the simulation test is shown in Table 7.

As for the crash speed of the UAV, considering that the limit height of the UAV in Singapore is 60 m, according to Newton's law and considering the influence of initial level flight speed, in our research, we set the crash speeds of UAVs to be 15 m/s, 25 m/s, and 40 m/s based on findings reported by Che Man et al. [24].

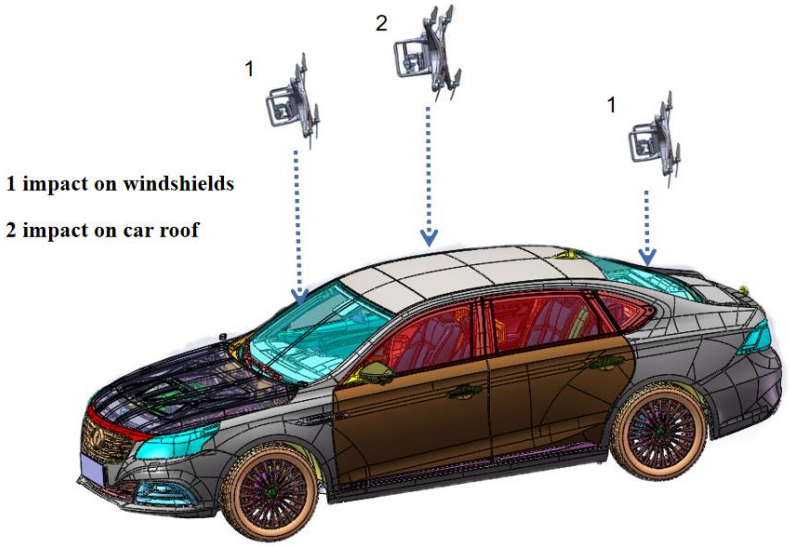

Fig. 7 Schematic diagram of sUAV impact on ground vehicles (modified from [15]).

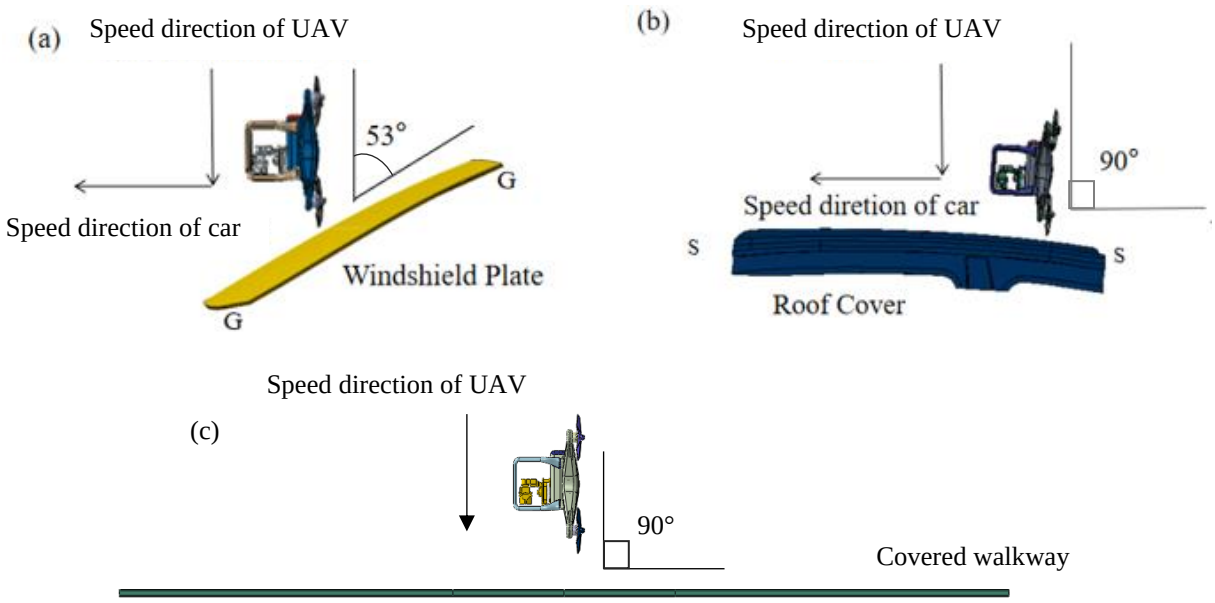

Fig. 8 FEA model assembly: (a) UAV and windshield assembly; (b) UAV and car roof cover assembly; and (c) UAV covered walkway assembly model.

Table 7 Collision simulation parameters (speed and angles)

Impact Location	**The crash speed of sUAV (m/s)**			**The forward speed of car (km/h)**			**Angle between plane and sUAV**
Car Windshield	15	25	40	30	50	90	53°
Car Roof	40		50	30	50	90	90°
Covered Walkway	40		50	-	-	-	90°

IV. Results and Discussions

In this section, the influence of the UAV impact positions, as well as the impact velocity on the damage results of the car model, will be studied. As discussed in this section, we will analyze the influence of two collision configurations (i.e., impact on windshield glass and impact on a steel plate), three UAV crashing speeds (i.e., 10 m/s, 25 m/s, 40 m/s), and three driving car speeds (i.e., 30 km/h on the slow road, 50 km/h on the road, 90 km/h on the highway).

A. Impact on car windshield

In this subsection, the collision simulation of the laminated glass used in the simulation was carried out with different collision speeds and collision angles. The simulation results are as follows.

In this section, the influence of sUAV crash speed, car forward speed, impact position and angle on the dynamic response and damage severity level of the car windshield will be studied. As presented in Fig. 9, Fig. 10, and Fig. 11, the damage to car windshield and contact forces for sUAV crash speeds of 15 m/s, 25 m/s and 40 m/s, respectively, for car forward speeds of 50 km/h and 90 km/h were considered.

The result shows a clear relation between car forward speed (kinetic energy) with car windshield damage, it is clear that for car forward speed of 50 km/h, the sUAV crash inflicts limited damage to car windshield, while some cracks on car windshield damage can found for sUAV crash at car forward speed of 90 km/h. The influence of sUAV crash speed is more dominant at higher speed where the crack pattern growth at crash speed of 25 m/s is extensive compared to crash speed of 15 m/s.

Outside Vehicle	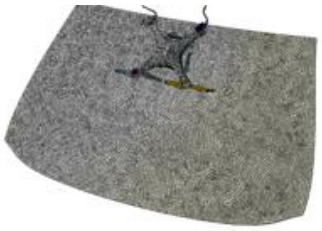	
Inside Vehicle		
Car forward speed	(a) 50 km/h	(a) 90 km/h

Fig. 9 Damage to car Windshield for car forward speed: 50 km/h and 90 km/h (sUAV crash speed of 15 m/s at 90°).

When the crash speed of the UAV was 40m/s, on low-speed roads, the UAV can only cause limited damage and cracks to the windshield, as shown in Fig. 11, but on the normal road (vehicle speed is 50 km/h) and highways (vehicle speed is 90 km/h) had caused serious damage to the windshield, and the visibility of the windshield was almost completely lost, as shown in Fig. 12. The front view of the crack propagation process of the UAV hitting the windshield within 0-15 ms is shown in Fig. 12. The crack had almost spread to the entire department, while the camera had achieved penetration into the windshield, and the overall windshield was deformed more seriously.

Select the low-speed, medium-speed, and high-speed impacts. The time point for the peak of contact force is similar to the head impact experiment mentioned above. The experimental result by Sang et al. [25] showed that the peak contact force appeared later, as shown in Fig. 13. This may be caused by the difference between vertical impact and horizontal impact, and the overall wave shapes of our study and its study are relatively similar.

Outside Vehicle			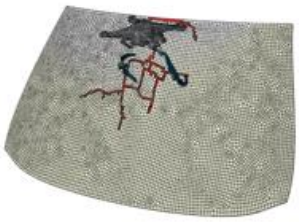
Inside Vehicle			
Car forward speed	(a) 30 km/h	(a) 50 km/h	(a) 90 km/h

Fig. 10 Damage to car Windshield for car forward speed: 30 km/h, 50 km/h and 90 km/h (sUAV crash speed of 25 m/s at 90°).

Outside Vehicle	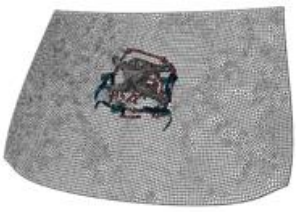		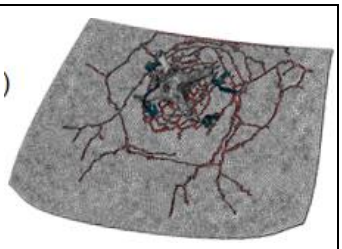
Inside Vehicle	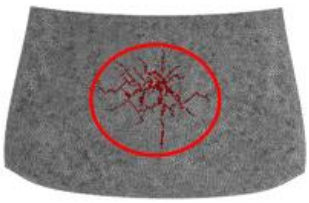	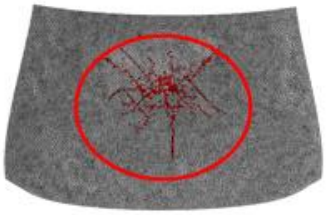	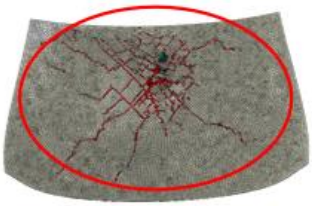
Car forward speed	(a) 30 km/h	(a) 50 km/h	(a) 90 km/h

Fig. 11 Damage to car Windshield for car forward speed: 30 km/h, 50 km/h and 90 km/h (sUAV crash speed of 40 m/s at 90°).

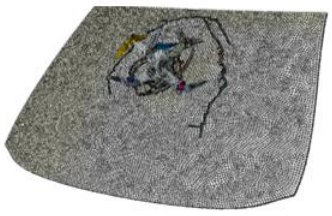	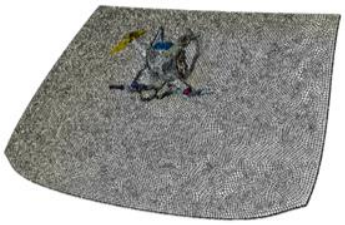	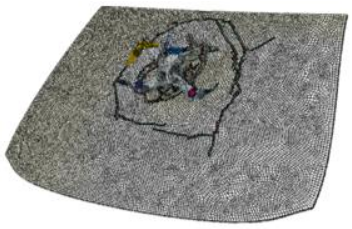
t = 1.25 ms	t = 2.50 ms	t = 3.75 ms
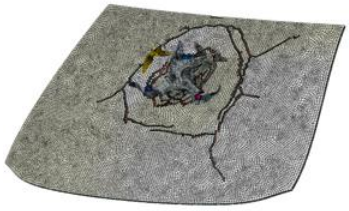	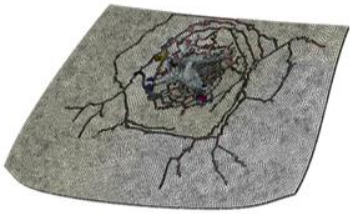	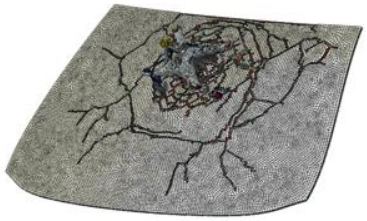
t = 5 ms	t = 10 ms	t = 15 ms

Fig. 12 Damage to car Windshield for car forward speed: 90 km/h (sUAV crash speed of 40 m/s).

B. Impact on steel plate (car roof)

In this subsection, the collision simulation of the steel plate used in the simulation was carried out with different collision speeds. The simulation results include the sUAV crash process, stress contour and force history are presented as follows.

When the sUAV crash velocity is 40m/s, and the relative velocity of the car is 90 km/h (25 m/s), the sUAV cannot realize the penetration of the steel plate; even at a higher sUAV crash speed of 50 m/s, there was no significant difference as shown in Fig. 14. The max stress occurs at 2.5ms when the UAV crash velocity is 40 m/s and the relative velocity of the car is 25 m/s as shown in Fig. 15, the deformation of the top steel plate of the car is mainly concentrated near the impact point.

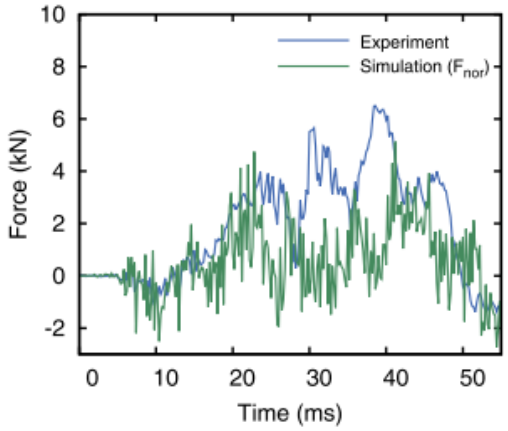

(a) Experimental force-time data [25]

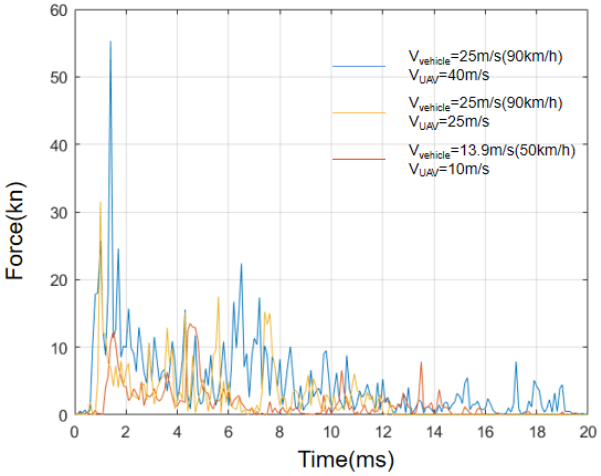

(b) Present simulation force-time data for Collision speeds of high, middle, and low.

Fig. 13 Impact force-time history data in the experiment [25] and present simulation.

In these cases, the deformation of the sUAV body and landing gear is more serious. Although the steel plate has large-area stress changes at the impact speed of 50m/s, there is no damage under the impact at various speeds. The contact force for the cases when the sUAV crash velocity is 40 m/s in two different car speed conditions are compared and shown in Fig. 15(b). In addition, Fig. 15 also compares the contact force of the roof steel plate under different road conditions. Numerical results show that in the case of the same crash, the speed of the car has a significant effect on the contact force, the peak value is larger in the highway and ordinary road segments. In addition, the peak contact force in different flight phases occurs at different times, mainly due to the difference between the initial speed of the 3 different phases. The initial speed of the highway road segment is the largest, which will result in the earliest peak, followed by the ordinary road segment and the low-speed section. In addition, we can observe that there are multiple peaks in three cases. This multi peak phenomenon is because the drone is a typical non-uniformity composed of different stiffness, and the top steel plate throughout the car may be affected by different components during the impact process.

	t = 0 ms	t = 10 ms	t = 15 ms
V_{UAV}=40 m/s	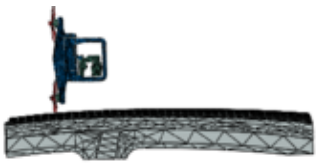		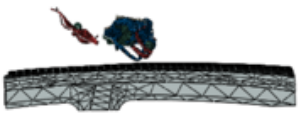
V_{UAV}=50 m/s	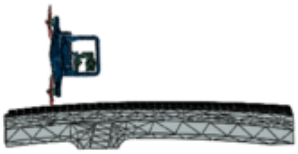	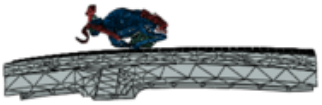	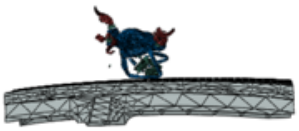

Fig. 14 Simulation results of drone impact on a steel plate for car forward speed at highway: 90 km/h (sUAV crash speed of 40 m/s and 50 m/s).

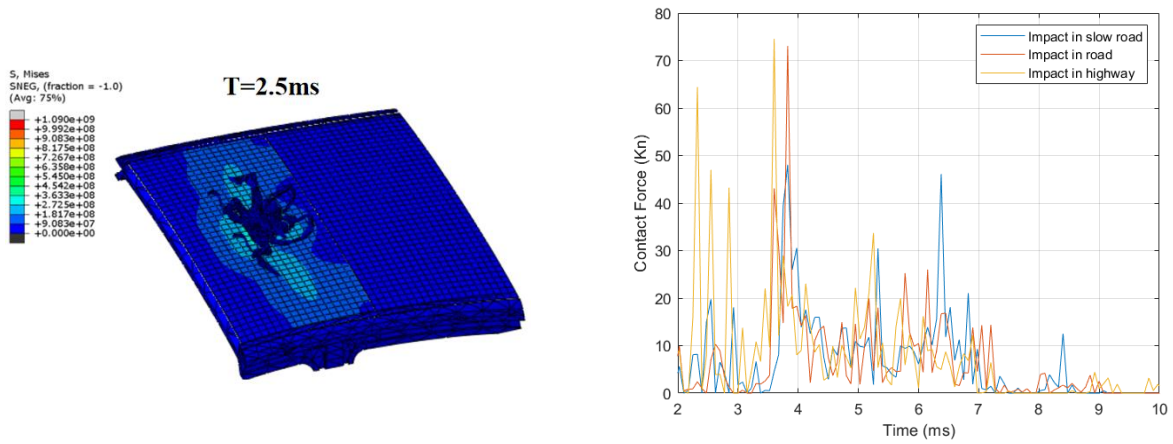

Fig. 15 Simulation results of sUAV impact on steel plate (a): Stress distribution for collision speed of V_{uav}=50m/s, $V_{vehicle}$= 25m/s at time = 2.5 ms, (b) force-time data for collision speeds of high, middle, and low.

C. Impact on covered walkway

In this subsection, the simulation of sUAV crash on aluminum honeycomb panel (covered walkway) was carried out at two different crash speeds, 40 m/s and 50 m/s. When the sUAV crash on covered walkway at velocity of 40m/s, a large deformation can be observed without penetration on the aluminum honeycomb panel, even at higher sUAV crash speed of 50 m/s shows no significant difference as depicted in Fig. 16. It was noted covered walkway is under larger deformation compared to car roof because of aluminum lower stiffness in nature, which indicate the covered walkway require thickness more than 10 mm to provide better protection against crash with heavier and faster UAV.

The highest reaction force occurs at t = 10 ms for sUAV crash velocity of 50 m/s as shown in Fig. 17(a), because at t = 10 ms, the sUAV front arm, motor and main body have reached the panel to exert full load from the crash. Followed by reduction in reaction force after the crash, where the crash energy is absorbed by panel large deformation. Closer look at stress the deformation of the aluminum honeycomb panel of the covered walkway is mainly concentrated near the impact point as shown in Fig. 17(b). The deformation process shows no penetration from sUAV collision with steel plate (car roof) and crash on aluminum panel (covered walkway) compared to collision on the car windshield. Higher energy absorption in metal material through large deformation indicate car roof and covered walkway provide better crash protection against small UAV less than 2 kg.

	t = 0 ms	t = 10 ms	t = 15 ms
V_{UAV}=40 m/s	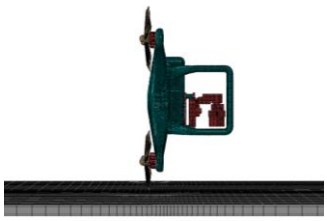		
V_{UAV}=50 m/s		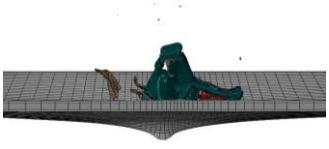	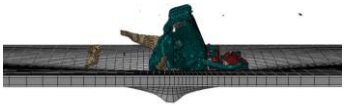

Fig. 16 Simulation results of drone impact on aluminum honeycomb panel for sUAV crash speed of 40 m/s and 50 m/s.

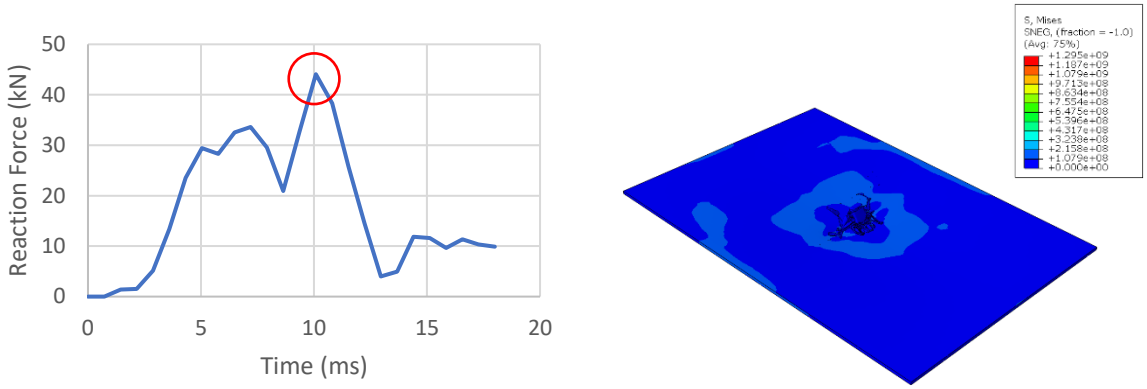

Fig. 17 Simulation results of sUAV impact on aluminum honeycomb panel: (a) reaction force history for sUAV crash speed of V_{uav}=50m/s, (b) Stress distribution for crash speed of V_{uav}=50m/s, at time = 10 ms.

V. Concluding Remarks and Future Works

Based on the finite element simulation, this paper investigate the influence collision of small UAV to the ground vehicles and covered walkway, as well as estimate the impact of the sUAV collision on the damage of the ground vehicles on different road conditions.

It is found the damage severity level of car windshield due to drone crash at higher car forward speed cause more severe damage for the same weight category. Although no penetration found from the sUAV crash on car windshield up to speed 40 m/s. However, the crack that cover car windshield reduce driver visibility and potentially led to traffic accident. Similarly, no penetration can be observed for sUAV collision on car roof and crash on covered walkway for sUAV crash speed up to 50 m/s due to crash energy absorption by the metal structure through large deformation which indicate car roof and covered walkway provide better crash protection against small UAV less than 2 kg.

From the simulation results, we can roughly conclude that within the crash speed range of the sUAV, the speed between 25 m/s - 40 m/s can be used as the critical speed for crossing the front windshield, side windows and other parts of the vehicle. Below this speed, the UAV cannot effectively pass through the car windshield, car roof and covered walkway and pose very minimal threat to driver and pedestrian safety.

This paper is a primary attempt to estimate damage to the ground vehicles due to collision with the sUAV, by using the simulation results collision severity of ground vehicles caused by UAV collision, only one type of UAV and simplified components of the vehicles are considered in the study. In addition, the present simulation works limited to sUAV with weight less than 2 kg, which are not sufficient to draw conclusive conclusions. Therefore, further analysis with various crash parameters (e.g., impact location, different UAV crash speed, crash angle, and weight categories) will be further explored in the future works.

More studies on the different type of vehicles (family cars, subway, urban light rail, bus and so on) subjected to the strike of UAV with different categories can be further performed to build the risk matrix of UAV ground collision to vehicles in future work. Insights from this study will guide aviation airworthiness authorities to better understand the damage severity level to ground vehicles and pedestrian due to sUAV collision. At the same time, this will facilitate aviation authorities to formulate regulations for safer sUAV operations.

Acknowledgement

This research is supported by the National Research Foundation, Singapore, and the Civil Aviation Authority of Singapore, under the Aviation Transformation Programme. Any opinions, findings and conclusions or recommendations expressed in this material are those of the authors and do not reflect the views of National Research Foundation, Singapore, and the Civil Aviation Authority of Singapore.

References

[1] F. A. A. (FAA), "Summary of small unmanned aircraft rule (Part 107)," in "Washington, DC: Federal Aviation Administration," 2016.

[2] E. Petritoli, F. Leccese, and L. Ciani, "Reliability assessment of UAV systems," *IEEE International Workshop on Metrology for AeroSpace (MetroAeroSpace) June 2017*, p. 5, 2017, doi: 10.1109/MetroAeroSpace.2017.7999577.

[3] S. E. Lee, J. W. Jung, Y. Choi, Y. J. Yoon, and J. W. Hong, "Unmanned Aerial Vehicle Impacts on Heat-Strengthened Glass," *IEEE Access*, vol. 7, pp. 104269-104278, 2019, doi: 10.1109/ACCESS.2019.2930277.
[4] J. X. Liren, "Finite element model and optimization of windshield based on pedestrian head protection," Doctoral dissertation, Harbin Institute of Technology.
[5] B. Liu, Y. Wang, X. Xu, W. Zhang, J. Xu, and Y. Li, "Experimental research on energy absorption characteristic of PVB laminated windshield subjected to headform low-speed impact," *J. Mech. Eng*, vol. 49, p. 128, 2013.
[6] E. A. S. Agency, "'Drone Collision' Task Force," 2016. [Online]. Available: https://www.easa.europa.eu/document-library/general-publications/drone-collision-task-force
[7] T. J. Holmquist, G. R. Johnson, C. M. Lopatin, D. E. Grady, and J. Hertel, E S, "High strain rate properties and constitutive modeling of glass," United States, 1995. [Online]. Available: https://www.osti.gov/biblio/41367
[8] G. Herndon, K. Allen, A. Roberts, D. Phillips, and S. A. Batzer, "Automotive side glazing failure due to simulated human interaction," *Engineering Failure Analysis*, vol. 14, no. 8, pp. 1701-1710, 2007/12/01/ 2007, doi: https://doi.org/10.1016/j.engfailanal.2006.11.070.
[9] M. Wingren, "Windscreen study using a free moving headform : An investigation of windscreen behaviour when subjected to headform impact," Independent thesis Advanced level (degree of Master (One Year)) Student thesis, 2011. [Online]. Available: http://urn.kb.se/resolve?urn=urn:nbn:se:his:diva-5382
[10] S. Zhao, L. R. Dharani, L. Chai, and S. D. Barbat, "Analysis of damage in laminated automotive glazing subjected to simulated head impact," *Engineering Failure Analysis*, vol. 13, no. 4, pp. 582-597, 2006/06/01/ 2006, doi: https://doi.org/10.1016/j.engfailanal.2004.12.038.
[11] J. Chen, J. Xu, X. Yao, X. Xu, B. Liu, and Y. Li, "Different driving mechanisms of in-plane cracking on two brittle layers of laminated glass," *International Journal of Impact Engineering*, vol. 69, pp. 80-85, 2014/07/01/ 2014, doi: https://doi.org/10.1016/j.ijimpeng.2014.02.014.
[12] "AIR NAVIGATION ACT (CHAPTER 6). AIR NAVIGATION (101 — UNMANNED AIRCRAFT OPERATIONS) REGULATIONS 2019.," ed. Singapore: CIVIL AVIATION AUTHORITY OF SINGAPORE (CAAS), 2019.
[13] J. Xu *et al.*, "Characteristics of windshield cracking upon low-speed impact: Numerical simulation based on the extended finite element method," *Computational Materials Science*, vol. 48, no. 3, p. 7, 2010, doi: https://doi.org/10.1016/j.commatsci.2010.02.026.
[14] B. Liu, T. Xu, X. Xu, YanWang, Y. Sun, and Y. Li, "Energy absorption mechanism of polyvinyl butyral laminated windshield subjected to head impact: Experiment and numerical simulations," *International Journal of Impact Engineering*, vol. 90, p. 11, 2016, doi: https://doi.org/10.1016/j.ijimpeng.2015.11.010.
[15] PCauto. "Illustrated Car." https://www.pcauto.com.cn/jingxuan/article/13/ (accessed.
[16] Azom, "AISI 4340 Alloy Steel (UNS G43400)," Sept 2012.
[17] H. Liu, M. H. Che Man, and K. H. Low, "UAV airborne collision to manned aircraft engine: Damage of fan blades and resultant thrust loss," *Aerospace Science and Technology*, vol. 113, p. 106645, 2021/06/01/ 2021, doi: https://doi.org/10.1016/j.ast.2021.106645.
[18] C. C. Foo, L. K. Seah, and G. B. Chai, "Low-velocity impact failure of aluminium honeycomb sandwich panels," *Composite Structures*, vol. 85, no. 1, p. 9, 2008, doi: https://doi.org/10.1016/j.compstruct.2007.10.016.
[19] H. Abaqus, "Karlsson and Sorensen Inc," *Theory manual–version*, vol. 6, 2001.
[20] L. T. Authority. "Driving in Singapore." https://www.lta.gov.sg/content/ltagov/en/getting_around.html#driving_in_singapore (accessed.
[21] J. V. Foster and D. Hartman, "High-Fidelity Multi-Rotor Unmanned Aircraft System (UAS) Simulation Development for Trajectory Prediction Under Off-Nominal Flight Dynamics," in *17th AIAA Aviation Technology, Integration, and Operations Conference*, 2017.
[22] C. Lum and B. Waggoner, "A Risk Based Paradigm and Model for Unmanned Aerial Systems in the National Airspace," in *Infotech@Aerospace 2011*, (Infotech@Aerospace Conferences: American Institute of Aeronautics and Astronautics, 2011.
[23] R. Aalmoes, Y. S. Cheung, E. Sunil, J. M. Hoekstra, and F. Bussink, "A conceptual third party risk model for personal and unmanned aerial vehicles," in *2015 International Conference on Unmanned Aircraft Systems (ICUAS)*, 9-12 June 2015 2015, pp. 1301-1309, doi: 10.1109/ICUAS.2015.7152424.
[24] M. H. C. Man, H. Haoliang, and K. H. Low, "Crash Area Estimation for Ground Risk of Small Unmanned Aerial Vehicles Due to Propulsion System Failures," presented at the AIAA SCITECH 2022 Forum, San

Diego, CA & Virtual, 2021. [Online]. Available: https://arc.aiaa.org.remotexs.ntu.edu.sg/doi/abs/10.2514/6.2022-1506.
[25] S. E. Lee, J.-W. Jung, Y. Choi, Y.-J. Yoon, and J.-W. Hong, "Unmanned Aerial Vehicle Impacts on Heat-Strengthened Glass," *IEEE Access*, vol. 7, p. 10, 2019, doi: https://doi.org/10.1109/ACCESS.2019.2930277.